The Cryosphere

Open Access

EGU

Supplement of

Potential faster Arctic sea ice retreat triggered by snowflakes' greenhouse effect

Jui-Lin Frank Li et al.

Correspondence to: Jui-Lin Frank Li (juilin.f.li@jpl.nasa.gov)

Table S1: List of CMIP5 models used in this study separated according to whether they simulate falling ice radiative effects (i.e. falling snow radiative effects on, SoN) or whether they do not simulate these effects (i.e. no falling snow radiative effects, NoS). All r1i1p1 simulations were considered that provide the necessary surface flux and sea ice fields for the scenarios of interest.

| CMIP5 models without FIRE (NoS)	CMIP5 Models with FIRE (SoN)
ACCESS1-0	GFDL-CM3
ACCESS1-3	GFDL-ESM2G
BNU-ESM	GFDL-ESM2M
CCSM4	GISS-E2-H
CESM1-BGC	GISS-E2-R
CNRM-CM5	HadGEM2-CC
CanESM2	HadGEM2-ES
FGOALS-g2	
IPSL-CM5A-LR	
IPSL-CM5A-MR	
IPSL-CM5B-LR	
MIROC-ESM	
MIROC-ESM-CHEM	
MPI-ESM-LR	
MPI-ESM-MR	
MRI-CGCM3	
NorESM1-M	
NorESM1-ME	

5

10

15

Table S2: Properties of the NSIDC sea ice extent time series noise structure by calendar month and for 1979—2005 and 1979—2017. In each case the statistics are performed on the residuals after removing an optimised least squares trend fit: the lag-1 Pearson correlation coefficient (r), the Ljung-Box p value for significant lag-1 autocorrelation and the Kolmogorov-Smirnov p value with a null hypothesis of Normal noise.

|	1979—2005			1979—2017		
	r	Ljung-Box p	Kolmogorov-Smirnov p	r	Ljung-Box p	Kolmogorov-Smirnov p
January	0.16	0.46	0.98	0.33	0.04	0.22
February	0.18	0.41	0.97	0.37	0.02	0.98
March	-0.06	0.74	0.49	0.18	0.25	0.83
April	0.14	0.46	1.00	0.28	0.07	1.00
May	0.04	0.81	0.25	0.12	0.45	0.91
June	-0.53	0.01	0.53	-0.12	0.42	0.72
July	-0.44	0.02	1.00	0.10	0.53	0.99
August	-0.30	0.12	0.53	0.15	0.34	0.95
September	-0.25	0.20	0.97	0.12	0.45	0.89
October	-0.14	0.52	1.00	0.15	0.34	0.30
November	0.08	0.65	0.92	0.10	0.56	0.86
December	0.30	0.10	0.22	0.35	0.03	0.96
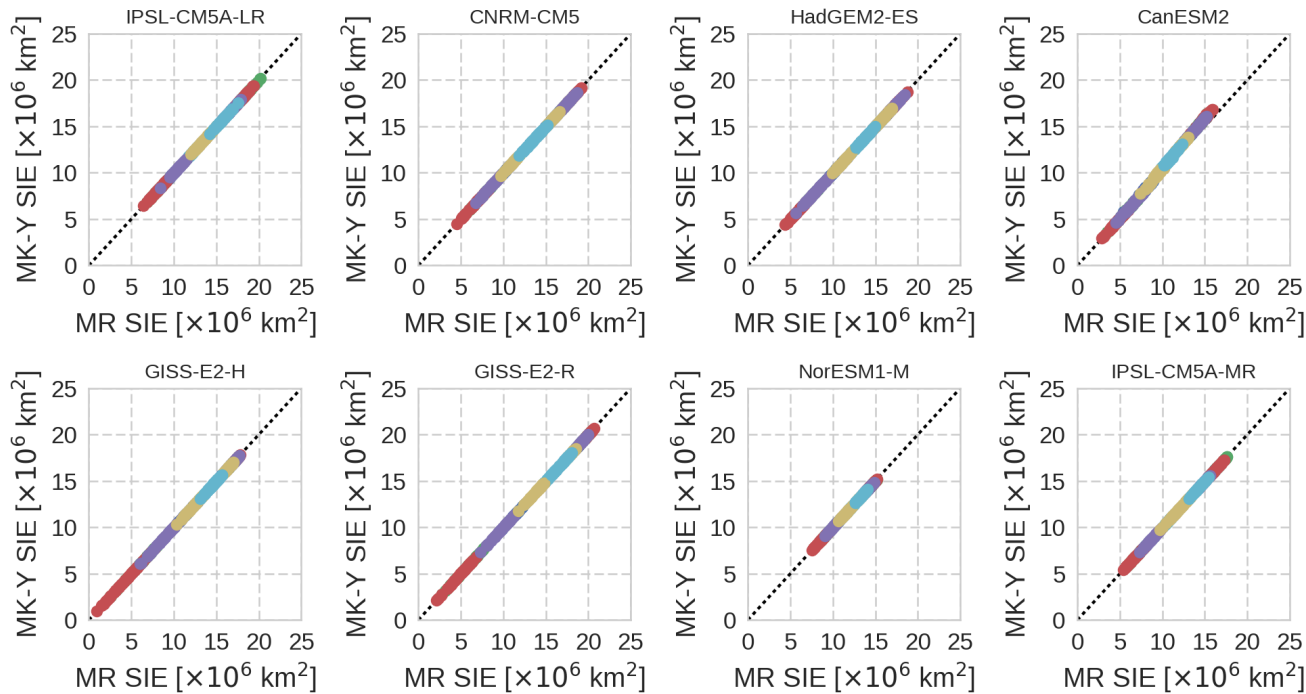
Figure S1: Month-by-month comparisons of calculated sea ice extent by the authors (MR SIE, x axis) and for the same values previously published (Kirchmeier-Young et al., 2017) for eight historical-RCP8.5 simulations over 1960—2020. Each calendar month is shown by a different colour and the 1:1 relationship is plotted as a black dotted line. Only models for which the Kirchmeier-Young outputs were provided are shown.
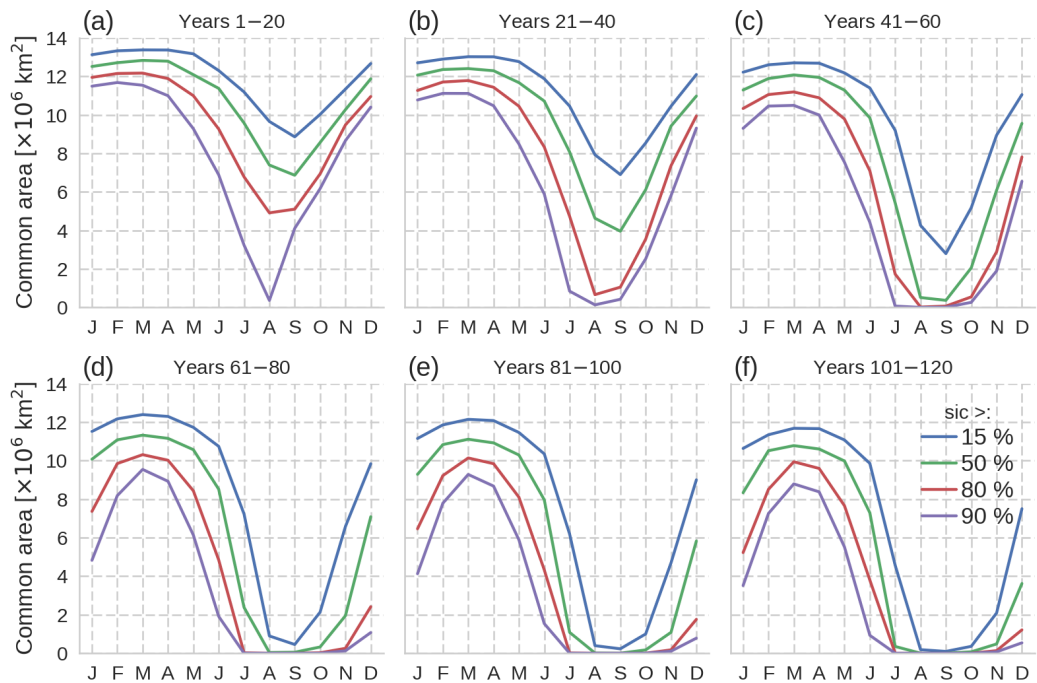
Figure S2: Area of ocean for which sea ice concentration exceeds a given threshold in both CESM1-SoN and CESM1-NoS when averaged for each calendar month over different 20-year periods under 1pctCO2. The colours refer to thresholds as labelled in the legend in (f). The common region that would be used for thickness calculations is similar to the minimum value in each line, e.g. from (a) the 90 % threshold would be limited by the August value $<1 \times 10^6$ km^2, whereas the 80 % threshold would cover >5 times as much ocean area.

4
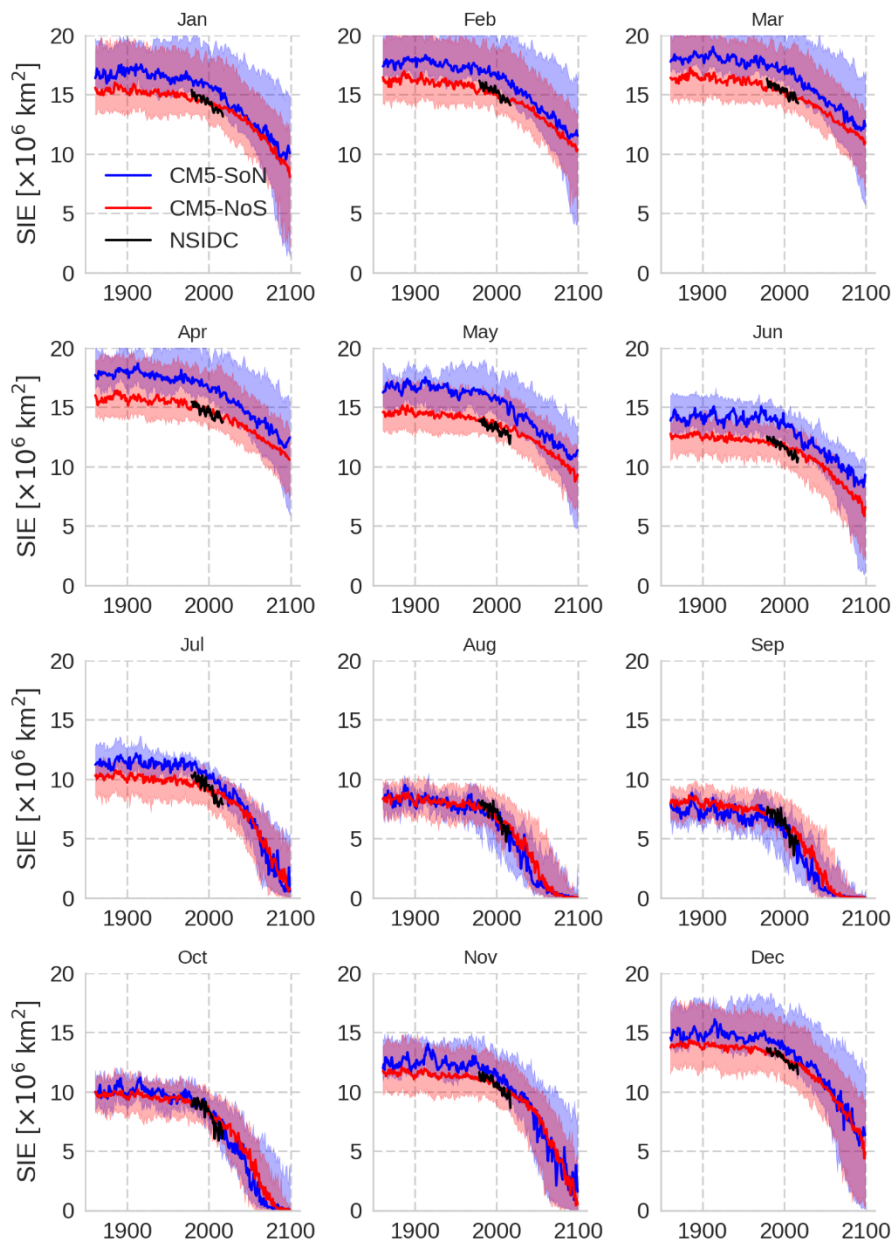
Figure S3: As main text Figure 1 except for sea ice extent changes in all calendar months. NSIDC observations in black, the CMIP5-NoS ensemble median and its 10—90 % range in red, and the same for the CMIP-SoN in blue.
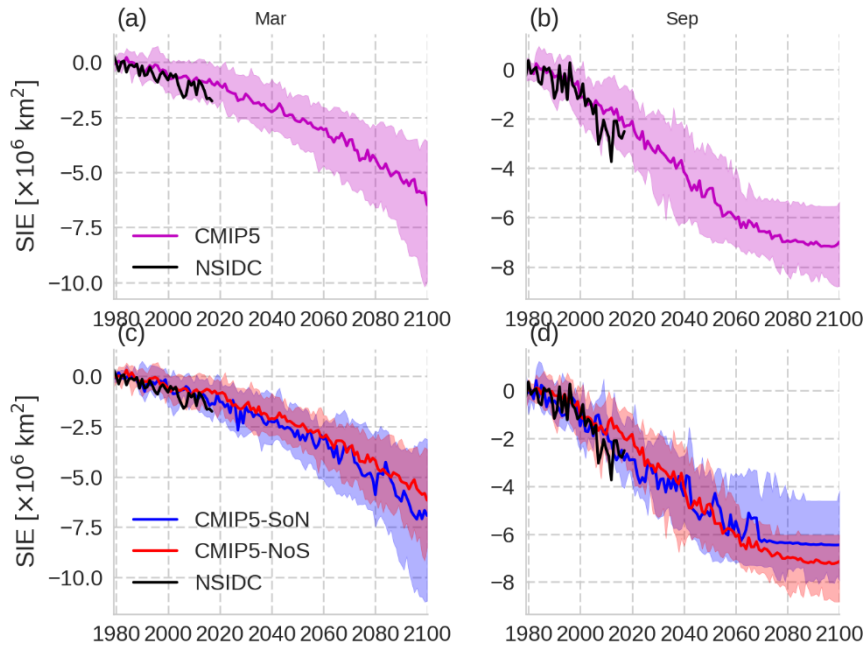
Figure S4: As main text Figure 1 except that SIE is presented as an anomaly relative to 1979—1984. Each CMIP5 simulation's anomaly is calculated relative to its own 1979—1984 value.
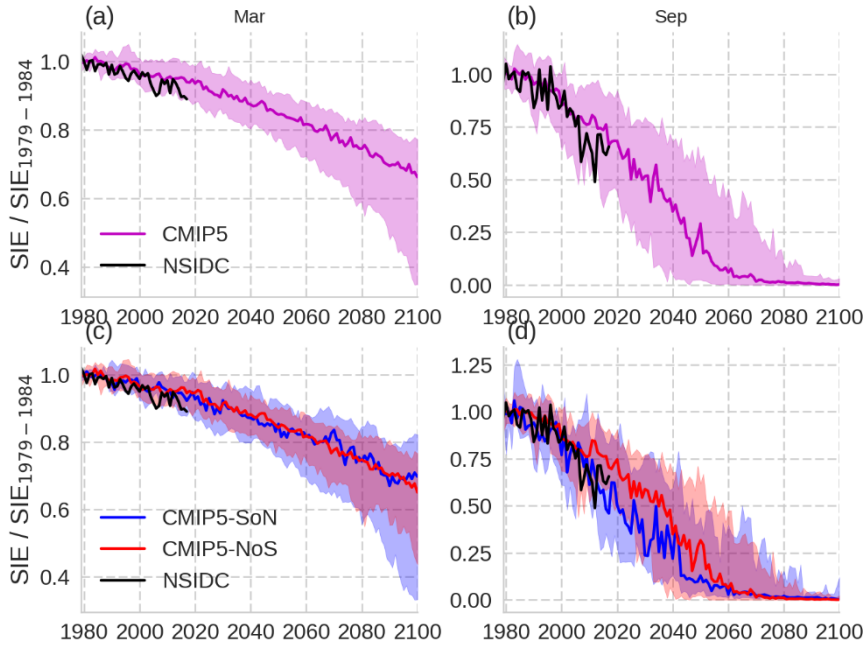
5   **Figure S5:** As main text Figure 1 except showing relative changes rather than absolute changes in SIE.
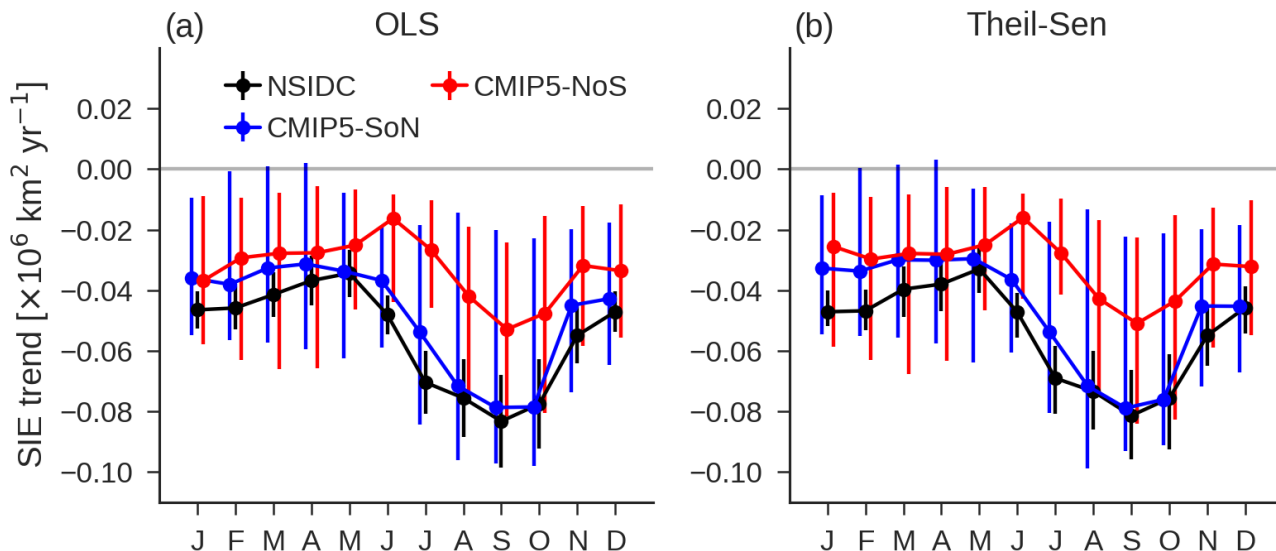
Figure S6. 1979—2017 trends calculated in NSIDC sea ice extent (black), the CMIP5-SoN ensemble (blue) and CMIP5-NoS ensemble (red). (a) trends from optimised least squares, error bars on observation are 2σ assuming white noise and on CMIP5 are the 95 % ensemble range and (b) trends from the Theil-Sen estimator where error bars on observations are the 95 % Theil-Sen range and on CMIP5 are the 95 % range of the individual model medians.
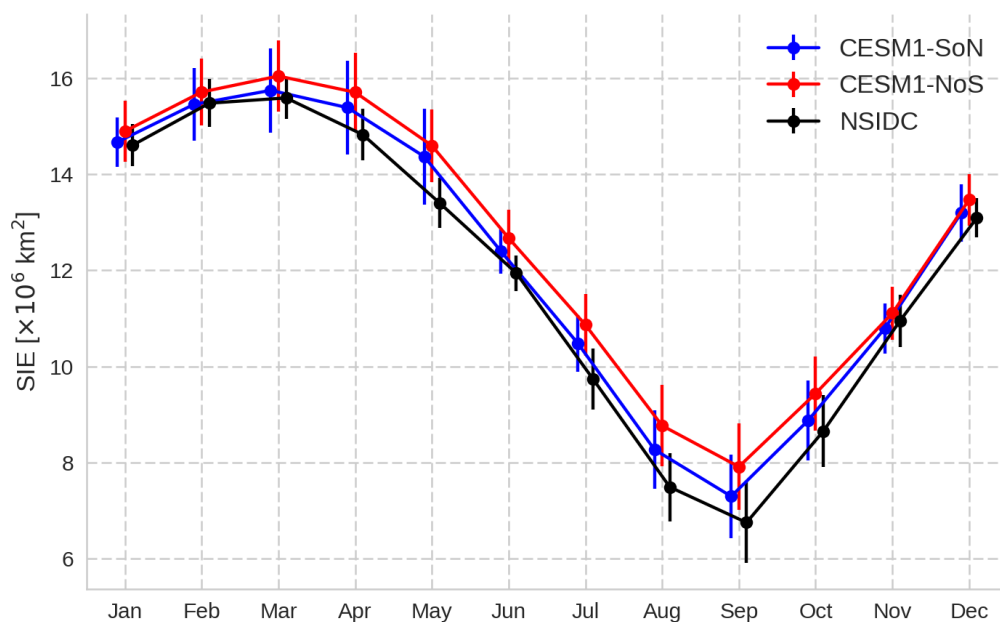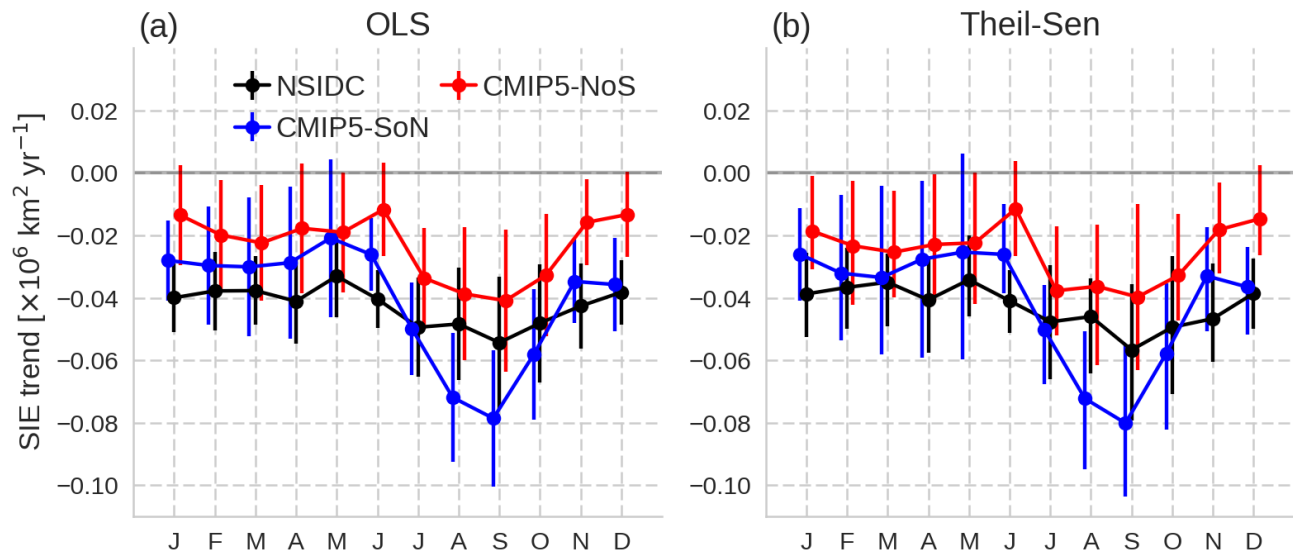

Figure S7: Mean annual cycle of sea ice extent over 1979—2005 in CESM1-SoN (blue), CESM1-NoS (red) and NSIDC observations(black). Error bars are 2 standard deviations of the detrended residuals to illustrate the magnitude of internal variability; the error in the mean is $\sqrt{27}$ times smaller. Points and bars are only offset sideways to prevent overlap.

Figure S8: Annual cycle of 1979—2005 trend in CESM1-SoN (blue), CESM1-NoS (red) and NSIDC observations (black solid). (a) estimate from OLS with ±2σ error estimates based on white noise and (b) Theil-Sen estimate with 95 % confidence intervals.